NEUROSCIENCE

Delta glutamate receptors are functional glycine- and D-serine–gated cation channels in situ

Elisa Carrillo[1], Cuauhtemoc U. Gonzalez[1,2], Vladimir Berka[1], Vasanthi Jayaraman[1,2]*

Delta receptors are members of the ionotropic glutamate receptor superfamily and form trans-synaptic connections by interacting with the extracellular scaffolding protein cerebellin-1 and presynaptic transmembrane protein neurexin-1β. Unlike other family members, however, direct agonist-gated ion channel activity has not been recorded in delta receptors. Here, we show that the GluD2 subtype of delta receptor forms cation-selective channels when bound to cerebellin-1 and neurexin-1β. Using fluorescence lifetime measurements and chemical cross-linking, we reveal that tight packing of the amino-terminal domains of GluD2 permits glycine- and D-serine–induced channel openings. Thus, cerebellin-1 and neurexin-1β act as biological cross-linkers to stabilize the extracellular domains of GluD2 receptors, allowing them to function as ionotropic excitatory neurotransmitter receptors in synapses.

INTRODUCTION

Excitatory neurotransmission in the mammalian central nervous system is primarily mediated by ionotropic glutamate receptors (*1*, *2*). This superfamily of ligand-gated ion channels includes *N*-methyl-D-aspartate (NMDA), α-amino-3-hydroxy-5-methyl-4-isoxazolepropionic acid (AMPA), and kainate receptors (*1*, *2*). Excitatory signaling is initiated by glutamate binding to these receptors, which thermodynamically triggers the opening of their cation-selective channels and causes depolarization of the neuron (*1*, *2*). Because of their sequence homology, the delta receptors, GluD1 and GluD2, are included in this family, but agonist-activated ion flux (channel gating) has not been observed in these putative ion channels (*3*). Nonetheless, delta receptors form trans-synaptic bridging complexes with the extracellular synaptic organizer molecule cerebellin-1 (Cbln1) and membrane-tethered presynaptic protein neurexin-1β (NRX1) (*4*–*7*), which has led to the suggestion that they play a structural role at synapses (fig. S1).

Despite the lack of evidence for direct agonist-mediated channel gating in delta receptors, their overall structure resembles other members of the superfamily (fig. S1) (*8*, *9*). In particular, their extracellular N-terminal and agonist-binding domains form a characteristic dimer-of-dimer assembly, with an agonist-binding cleft that closes upon glycine or D-serine binding (*10*–*13*). The GluD2 A654T ("Lurcher") mutant has been shown to form a constitutively active, cation-permeable channel (*12*–*15*). Ionotropic activity has also been observed in GluD2 upon activation of G_q-coupled metabotropic glutamate receptor with glutamate (*16*). The constitutive activity of GluD2 A654T Lurcher mutant and activation via the metabotropic glutamate receptor pathway has been shown to be blocked by a photoactivatable channel blocker attached to a cysteine near the channel pathway, further confirming the two pathways to be mediated by the GluD2 receptor channel (*17*). Because the agonist-binding and transmembrane domains of glutamate receptors can function independently, the lack of agonist-induced currents in wild-type delta receptors suggests that conformational changes in the agonist-binding domains cannot be transmitted to the transmembrane segments that form the channel pore. The N-terminal domains of delta receptors have unusually large conformational flexibility (*8*, *9*). Thus, the inter- and intradimer interactions that are critical for agonist-induced channel gating in AMPA and kainate receptors (*18*–*22*) may be energetically inaccessible in delta receptors. We hypothesize that, in the context of a synapse, where the N-terminal domains of delta receptors are constrained by Cbln1 and NRX1, dimeric interactions may be sufficient to allow these receptors to function as agonist-gated ion channels.

It is thus essential to investigate the ionotropic function of GluD2 receptors while maintaining the interactions with Cbln1 and NRX1 between the cells. To do this, we have performed the electrophysiology with cell clusters (Fig. 1A). The clusters allow for extensive contacts between the cells and for the associated protein-protein interactions. Under these conditions, we demonstrate that glycine and D-serine, but not glutamate, do support channel gating and cation influx in the GluD2 homomeric receptors. Consistent with our premise, this agonist-dependent gating required both Clbn1 and NRX1. To determine the conformational change underlying the GluD2 activity, we performed fluorescence lifetime imaging (FLIM) of these clusters. These studies show tighter packing of the N-terminal domain in the glycine-bound GluD2 in the presence of Clbn1 and NRX1. This finding is consistent with our premise that conformational restriction modulates the efficiency of glycine- or D-serine–mediated channel gating. To further support this inference, we limited conformational flexibility of the N-terminal domain by chemical cross-linking with cross-linkers of different lengths. Glycine-mediated channel opening was observed for short but not long cross-linkers. Glycine- and D-serine–gated currents were also observed in GluD2-rich cultured neurons from cerebellum in the presence of synaptic connections. These studies show that delta receptors function as glycine- and D-serine–gated ion channels in the context of synapses and open the door for further understanding and future targeting of these receptors implicated in a large number of neurological diseases.

RESULTS

To study GluD2 receptor gating in the presence of Cbln1 and NRX1, we performed electrophysiology in human embryonic kidney (HEK)–293T cell clusters following transient expression of the proteins. By recording from clusters of cells, we were able to study GluD2

[1]Center for Membrane Biology, Department of Biochemistry and Molecular Biology, University of Texas Health Science Center at Houston, 6431 Fannin St., Houston, TX 77030, USA. [2]MD Anderson Cancer Center UTHealth Graduate School of Biomedical Sciences, University of Texas Health Science Center at Houston, 6431 Fannin St., Houston, TX 77030, USA.
*Corresponding author. Email: vasanthi.jayaraman@uth.tmc.edu

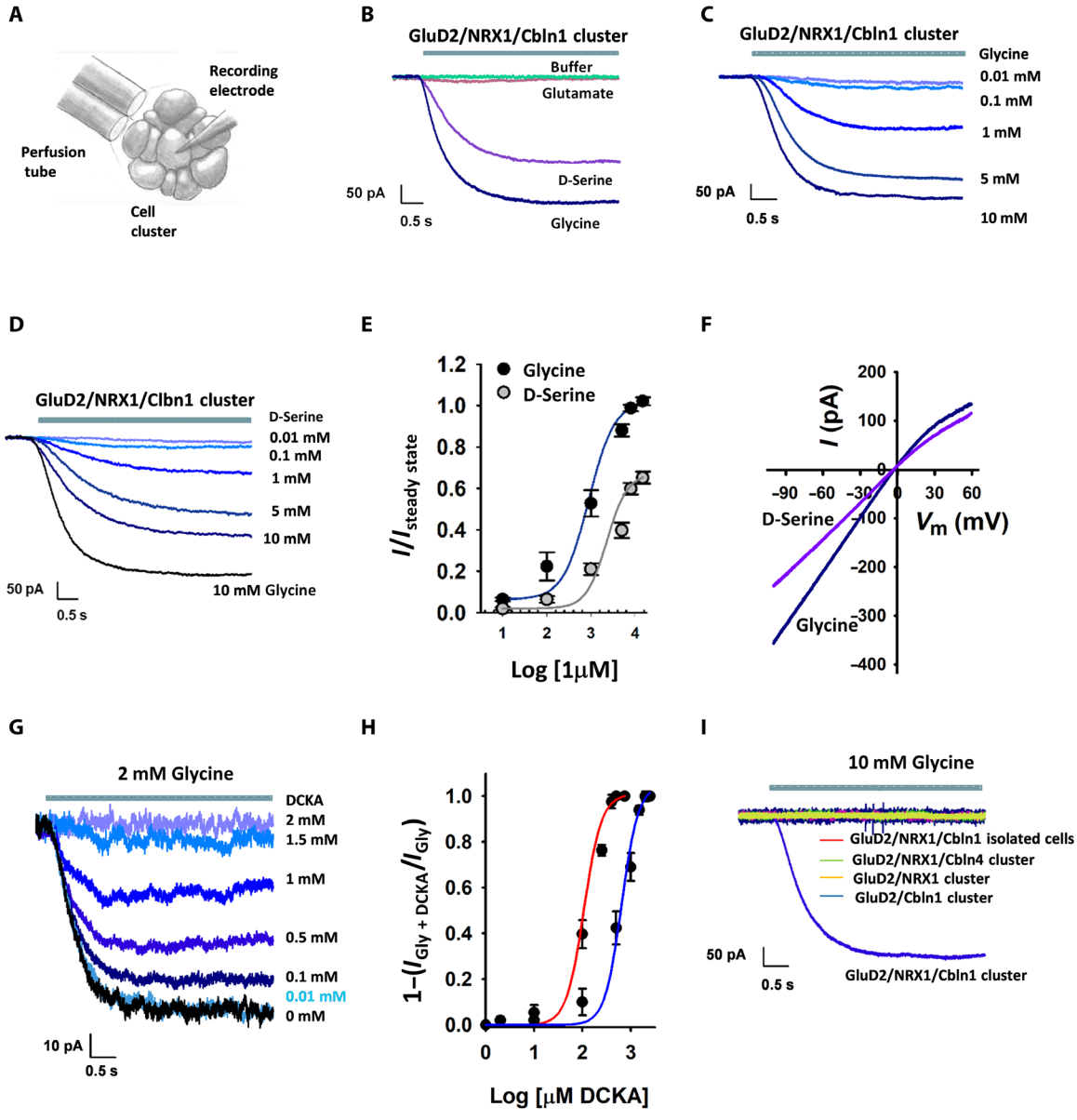

Fig. 1. Cbln1, NRX1, and cell-to-cell contacts are required for agonist-dependent gating of delta receptors. (**A**) Schematic drawing of HEK-293T cell cluster recordings. (**B** to **E**) Electrophysiological measurements of cells expressing GluD2, Cbln1, and NRX1. Representative currents activated by (B) 10 mM glycine, D-serine, glutamate, or no ligand (buffer); (C) different concentrations of glycine; and (D) different concentrations of D-serine. (E) Normalized concentration-response curves for glycine (EC_{50} = 1.07 ± 0.06 mM) and D-serine (EC_{50} = 2.9 ± 0.13 mM); number of measurements for each concentration is provided in table S1. (**F**) Current-voltage (*I-V*) relationship for glycine- and D-serine–mediated currents. (**G**) Representative currents showing inhibition of 2 mM glycine-mediated currents by 500 μM DCKA. (**H**) Normalized concentration-response curves showing DCKA inhibition with 500 μM glycine (red) and 2 mM glycine (blue); the number of measurements for each concentration is provided in table S1. (**I**) Glycine-activated currents in cells expressing GluD2 with either Cbln1 or NRX1 in clusters, Cbln4 and NRX1 in clusters, or Cbln1 and NRX1 in isolated cells compared to GluD2 with Cbln1 and NRX1 in clusters.

receptor function in the context of cell-to-cell contacts (Fig. 1A and fig. S2). In the presence of both Cbln1 and NRX1, glycine and D-serine activated inward currents at −60 mV, consistent with agonist-dependent gating of GluD2 receptor channels (Fig. 1B and fig. S3). In contrast, glutamate did not produce substantial currents, suggesting that, unlike most other family members, GluD2 receptors are not gated by glutamate (Fig. 1B). Concentration-response curves showed a median effective concentration (EC_{50}) value of 1.07 ± 0.06 mM and 2.9 ± 0.13 mM for glycine and D-serine, respectively (Fig. 1, C to E). The currents mediated by glycine also showed slight inward rectification (Fig. 1F). We also tested whether 5,7-dichlorokynurenic acid (DCKA), a competitive antagonist at the glycine site in NMDA receptors, would act as a competitive antagonist of the GluD2 receptors. Previous structure-function studies have shown that the closely related 7-chloro-4-oxo-1*H*-quinoline-2-carboxylic acid (7CKA) binds to the GluD2 agonist-binding domain and favors a more open cleft and that both 7CKA and DCKA lower the inhibition induced by D-serine in the GluD2 A654T Lurcher mutation, suggesting that

these compounds may act as competitive inhibitors (*11*). We observed that the currents obtained from GluD2 receptors in clusters in the presence of Cbln1 and NRX1 with glycine were inhibited by DCKA (Fig. 1G). The inhibition-concentration response curves for glycine-mediated currents with varying concentrations of DCKA was shifted to higher concentrations when the glycine concentration was increased, suggesting that DCKA could act as a competitive antagonist at the GluD2 receptors (Fig. 1H). Currents obtained from GluD2 receptors in clusters in the presence of glycine were not inhibited by pentamidine, a channel blocker of GluD2 A654T mutant, but showed a slight potentiation (fig. S4). This could be an allosteric effect similar to what is seen with spermine potentiation of the closely related GluN1/GluN2B subtype of NMDA receptor subtype (*23*, *24*). However, we cannot rule out other off target effects, as pentamidine binds to several cellular targets (*25*–*28*).

Glycine-activated currents were not observed when GluD2-, NRX1-, and Cbln1-expressing HEK-293T cells were studied in isolation (Fig. 1I and fig. S3), revealing the functional necessity of cell-to-cell contacts. In addition, both NRX1 and Cbln1 were required for glycine-activated currents, and Cbln4 failed to substitute for Cbln1 (Fig. 1I and fig. S3). Together, these observations indicate that agonist-dependent gating of GluD2 requires both Cbln1 and NRX1.

The GluD2 A654T Lurcher mutation gives rise to constitutively active channels that are inhibited by both glycine and the channel blocker pentamidine (Fig. 2A) (*14*, *15*). To examine whether Cbln1 and NRX1 affect the gating of Lurcher channels, we studied clusters of cells expressing this mutant in the absence (Fig. 2B and fig. S4) and presence (Fig. 2C and fig. S4) of Cbln1 and NRX1. Pentamidine inhibited currents in both conditions, but glycine inhibited currents only in the absence of Cbln1 and NRX1 (Fig. 2). In the presence of Cbln1 and NRX1, glycine potentiated the activity of the A654T mutant (Fig. 2C). These results suggest that Cbln1- and NRX1-mediated cell-to-cell contact primarily alters agonist-induced conformational changes. Specifically, inhibition of Lurcher channels by glycine in the absence of Cbln1 and NRX1 indicates that glycine binding causes desensitization (channel closure in the presence of agonist) of the constitutively open protein. Conversely, potentiation of Lurcher channel activity by glycine in the presence of Cbln1 and NRX1 suggests that the agonist further stabilizes constitutively open channels. A similar agonist-induced increase in activation and decrease in desensitization has been observed in AMPA receptors following mutation of the homologous alanine to threonine (*29*). We therefore propose that Cbln1 and NRX1 render the energetics of GluD2 similar to those in other members of the ionotropic glutamate receptor family, thus permitting agonist-induced activation.

Having established that Cbln1- and NRX1-mediated cell-to-cell contact can induce glycine-activated currents through GluD2 receptors, we sought to determine whether these currents are physiologically relevant. We isolated neurons from rat cerebellum, where GluD2 receptor expression is high (*30*), and rat cortex, where both GluD2 and GluD1 receptor expression is low (*30*). Following culture for 20 to 30 days to allow extensive neuronal contacts to be formed (fig. S7), synaptic connections were confirmed by spontaneous excitatory postsynaptic currents (EPSCs) and spontaneous action potentials. Under these conditions, both glycine and D-serine gave rise to robust currents in cerebellar neurons (Fig. 3A), while glutamate produced significantly smaller currents. We surmised that these currents were mediated by delta receptors, as the experiments were performed in the presence of inhibitors for AMPA and kainate receptors [10 μM (2,3-dioxo-6-nitro-7-sulfamoyl-benzo[f]quinoxaline) (NBQX)], NMDA receptor [100 μM DL-2-amino-5-phosphonovaleric acid (DL-AP5)], glycine receptor (1 μM strychnine), GABA receptor (10 μM bicuculline), and sodium channels (1 μM tetrodotoxin). Glycine-induced currents were much smaller in magnitude in cortical neurons than in cerebellar neurons (Fig. 3B), in agreement with the difference in delta receptor expression. No appreciable currents were observed when cerebellar neurons were studied in the absence of connections (Fig. 3B and fig. S2), confirming our earlier observation that cell-to-cell contact is essential for glycine-induced GluD2 gating in HEK-293T cells. The glycine concentration-response curve in cerebellar neurons (Fig. 3, C to E) was also similar to that observed in Cbln1-, NRX1-, and GluD2-expressing HEK-293T cell clusters (Fig. 1E), supporting our conclusion that these currents are primarily mediated by GluD2 receptors. In addition, glycine-mediated currents were inhibited by DCKA (Fig. 3D), the extent of inhibition was similar to what was observed for GluD2 receptors in clusters in the presence of Cbln1 and NRX1 (fig. S5), and pentamidine slightly potentiates the currents in neurons similar to that seen for GluD2 receptors in clusters in the presence of Cbln1 and NRX1 (fig. S4).

To investigate the conformational changes induced by Cbln1 and NRX1 that permit GluD2 to be gated by agonist, we measured fluorescence lifetimes of fluorophores introduced to the N-terminal domain of GluD2 expressed in isolated HEK-293T cells. We used a soluble *N*-ethylmaleimide–sensitive factor attachment protein (SNAP) tag to introduce donor and acceptor fluorophores at position 302. This site was chosen, as it allows fluorescence resonance energy transfer (FRET) to occur between SNAP Alexa Fluor 546 (donor) and SNAP 649 (acceptor) fluorophores located on adjacent dimers at proximal sites but not between fluorophores within a dimer or on adjacent dimers at distal sites (Fig. 4A). The fluorescence lifetimes of donor and acceptor fluorophores on GluD2 in the presence and absence of Cbln1 and NRX1 had two components (Fig. 4, B and C). The longer lifetime of 3.2 ns was similar to isolated donor lifetimes (3.2 ± 0.05 ns) and was therefore assigned to a site out of range for

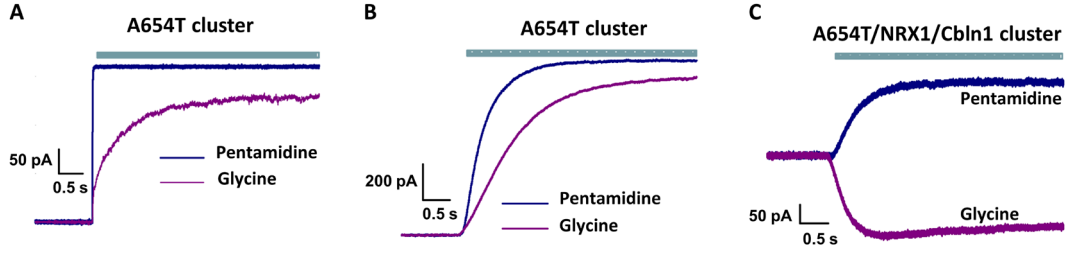

Fig. 2. Electrophysiological recordings with constitutively active GluD2 A654T mutant. Representative currents recorded upon application of 100 μM pentamidine or 10 mM glycine from (**A**) isolated cells, (**B**) cells in clusters in the absence of NRX1 and Cbln1, and (**C**) cell in clusters in the presence of NRX1 and Cbln1.

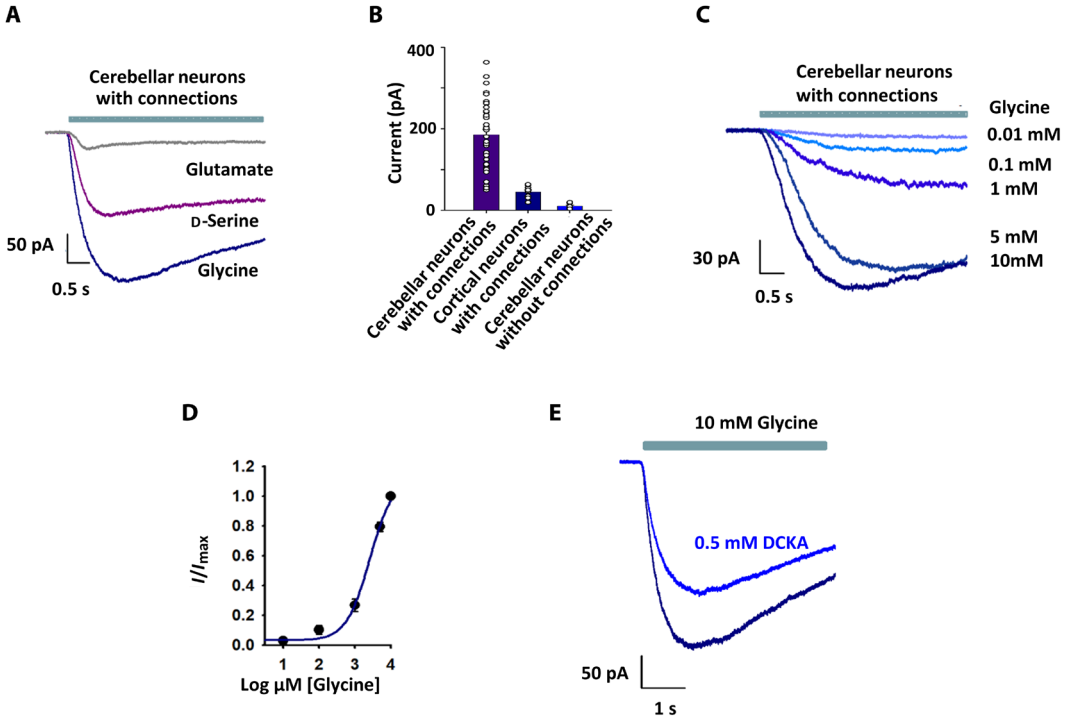

Fig. 3. Agonist activation of rat primary neuron delta receptors resembles that of GluD2 with Cbln1 and NRX1 in HEK-293T cell clusters. (**A**) Representative currents recorded from cerebellar neurons with established connections upon application of 10 mM glutamate, D-serine, or glycine. (**B**) Comparison of glycine-activated currents in cerebellar neurons with connections, cortical neurons with connections, and cerebellar neurons without connections. (**C**) Representative responses of cerebellar neurons with connections to different concentrations of glycine. (**D**) Normalized glycine concentration-response curve for cerebellar neurons with connections (EC_{50} = 1.48 ± 0.08 mM); the number of measurements for each concentration is shown in table S1. (**E**) Representative currents showing inhibition of 10 mM glycine-mediated currents by 500 µM DCKA.

FRET to occur with the acceptor (Fig. 4C). The shorter lifetime, which thus represented FRET between dimers at proximal sites, was significantly shorter for GluD2 receptors expressed in the presence (0.84 ± 0.05 ns) than in the absence (1.05 ± 0.09 ns) of Cbln1 and NRX1 (Fig. 4D). According to the Forster equation, this shorter lifetime is indicative of shorter distances between the two fluorophores, suggesting that packing between dimers in GluD2 receptors is tighter in the presence of Cbln1 and NRX1. This tight packing could underlie the ability of the receptor to undergo agonist-induced activation.

We subsequently used chemical cross-linking to limit conformational flexibility of the N-terminal domain to confirm our inference that tighter packing underlies the ability of agonists to induce currents through delta receptors. Cysteine residues were introduced at position 276 on GluD2, and thiol-reactive methanethiosulfonate (MTS) compounds of different lengths were used to form cross-links between dimers. Position 276 was chosen, because the distance of 28 Å between the sites on adjacent dimers was significantly shorter than the distance of 57 Å between this residue within a dimer (Fig. 5A). These distances are for GluD2 [Protein Data Bank identification (PDB ID): 6lu9] modeled into the most compact GluD1 structure (PDB ID: 6kss). Following chemical cross-linking of GluD2 expressed in isolated HEK-293T cells, glycine application evoked single-channel currents with a mean conductance of 20 ± 2.3 pS (Fig. 5, B to E), within the range of other ionotropic glutamate receptor subtypes (7 to 50 pS). Glycine-induced whole-cell currents were rapidly activating and partially desensitizing when short cross-linkers were used (Fig. 5, B to D, and fig. S6). The shortest cross-linker 1,1-methanediyl bis-MTS (M1M) did not produce currents in wild-type GluD2 receptor without cysteine at position 276, and no currents were observed in the absence of the cross-linker in GluD2 receptors with cysteine at position 276 (fig. S6), thus showing that the currents mediated by the cross-linkers were specific to cross-linking at site 276. The rapid kinetics are more likely to reflect the gating mechanism of delta receptors than the slower kinetics observed in cell clusters. The slower kinetics in the cell-to-cell connections are probably influenced by slow solution exchange associated with recordings from cells attached to the dish, which is necessary for maintaining cell-to-cell contact. One reason we believe that the slow kinetics are due to solution exchange is because the recording with A654T mutants in the absence of cell-to-cell contact show rapid kinetics and in cell clusters show slower kinetics (Fig. 2, A and B). Both single-channel and whole-cell activity were inversely correlated with cross-linker length (Fig. 5, B to F). No currents were observed with linker M17M, whose length (25 Å) is approximately the same as the distance between residue 276 in adjacent dimers (28 Å) in the cryo–electron microscopy structures (*8*, *9*). Together, these data indicate that conformations in which the N-terminal domains are splayed apart represent inactive states of the receptor.

Having ascertained that the relative position of the N-terminal domains of delta receptors can either permit or inhibit channel gating, we sought to determine whether these domains are essential for agonist activation. Deletion of the N-terminal domain in GluD2 resulted in receptors that were gated by both glycine and D-serine (Fig. 5H), indicating that the agonist-binding, transmembrane, and

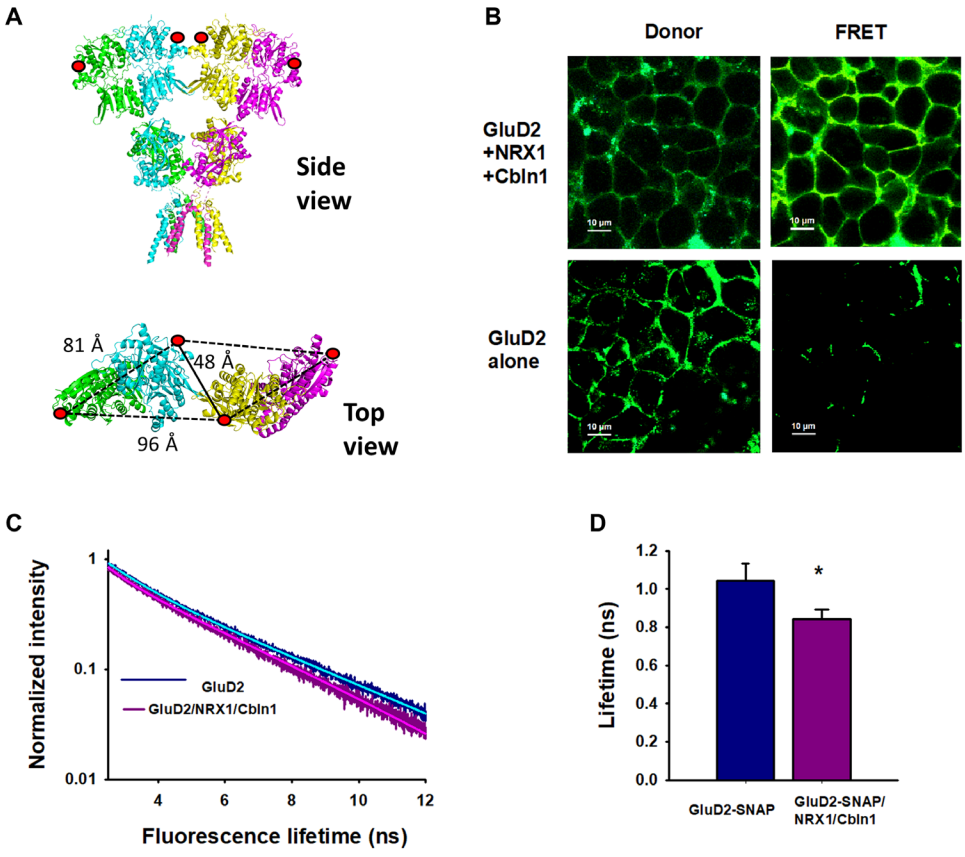

Fig. 4. Cbln1 and NRX1 induce tighter packing of the N-terminal domains of GluD2. (**A**) Structure of GluD2 (modeled on GluD1; PDB: 6KSS) showing SNAP tag incorporation at position 302 (red circles) and distance between dimers. Side view (top) and close-up top-down view of 302 N-terminal domain residues (bottom). (**B**) Fluorescent images of HEK-293T cells transfected with GluD2 alone or GluD2, NRX1, and Cbln1 showing the intensity of donor and FRET fluorescence. (**C** and **D**) Representative fluorescence lifetimes of donor- and acceptor-labeled cells expressing GluD2 alone or GluD2, Cbln1, and NRX1; solid lines show two exponential fits. (D) Donor lifetimes from at least three different days. Data represent mean lifetimes with SEs of the mean, $^*P = 0.00052$.

C-terminal domains are sufficient for ligand-gated ion channel function. To further confirm that the pathway is similar to that observed in GluD2, NRX1, and Cbln1 containing clusters and neurons, we show that these currents are inhibited to the same extent with DCKA as that seen with the other conditions (Fig 5I and fig. S5). The probability of opening for the GluD2 without the N-terminal domain is similar to that observed for the shortest cross-linker M1M, suggesting that the N-terminal domain may have an autoinhibitory effect on channel gating, stabilizing the desensitized state in the absence of trans-synaptic connecting proteins, and decreasing the likelihood of channel opening.

DISCUSSION

GluD2 receptors are predominantly expressed in Purkinje cells in the cerebellum and have been shown to be critical players in long-term depression (LTD), synapse formation, and motor coordination (*31*, *32*). Deletion of GluD2 in humans leads to cerebellar ataxia (*33*), atrophy, and upgaze (*34*), and alterations of GluD2 receptors have also been associated with schizophrenia (*35*) and depression (*36*).

Extensive insight has been gained into the role of specific domains of the GluD2 receptors in mediating LTD and synaptogenesis through investigations, where mutant GluD2 receptors have been genetically expressed into Purkinje cells in the GluD2 knockout mice. These studies have shown that the agonist-binding domain and C-terminal domain are critical in LTD, while the N-terminal domain is necessary for synapse formation (*37*, *38*). D-serine has been shown to be an endogenous ligand for the GluD2 receptors and reduces EPSCs due to an increase in endocytosis of AMPA receptors (*39*).

There is also indirect evidence for the involvement of the delta receptors in ionotropic excitatory signaling. Activation of metabotropic glutamate receptors was shown to lead to currents through GluD2 receptors in both heterologous expression system and in neurons (*16*). In addition, ionotropic activity has also been observed in the closely related GluD1 subtype. Pharmacological inhibition and genetic deletion of the GluD1 subtype of the delta receptor was shown to inhibit the ionotropic excitatory signaling in dorsal raphe nucleus (*40*). Selective knockdown of the GluD1 receptor in dorsal raphe nucleus resulted in anxiolytic behavior in the mice, conforming the physiological role of the ionotropic signaling of delta receptors. The ion channel activity of GluD2 has also been studied extensively with the constitutively active Lurcher mutant (*12*–*15*) and the ion channel activity mediated by activation of the metabotropic glutamate receptor pathway (*16*). Studies using chimeric receptors have

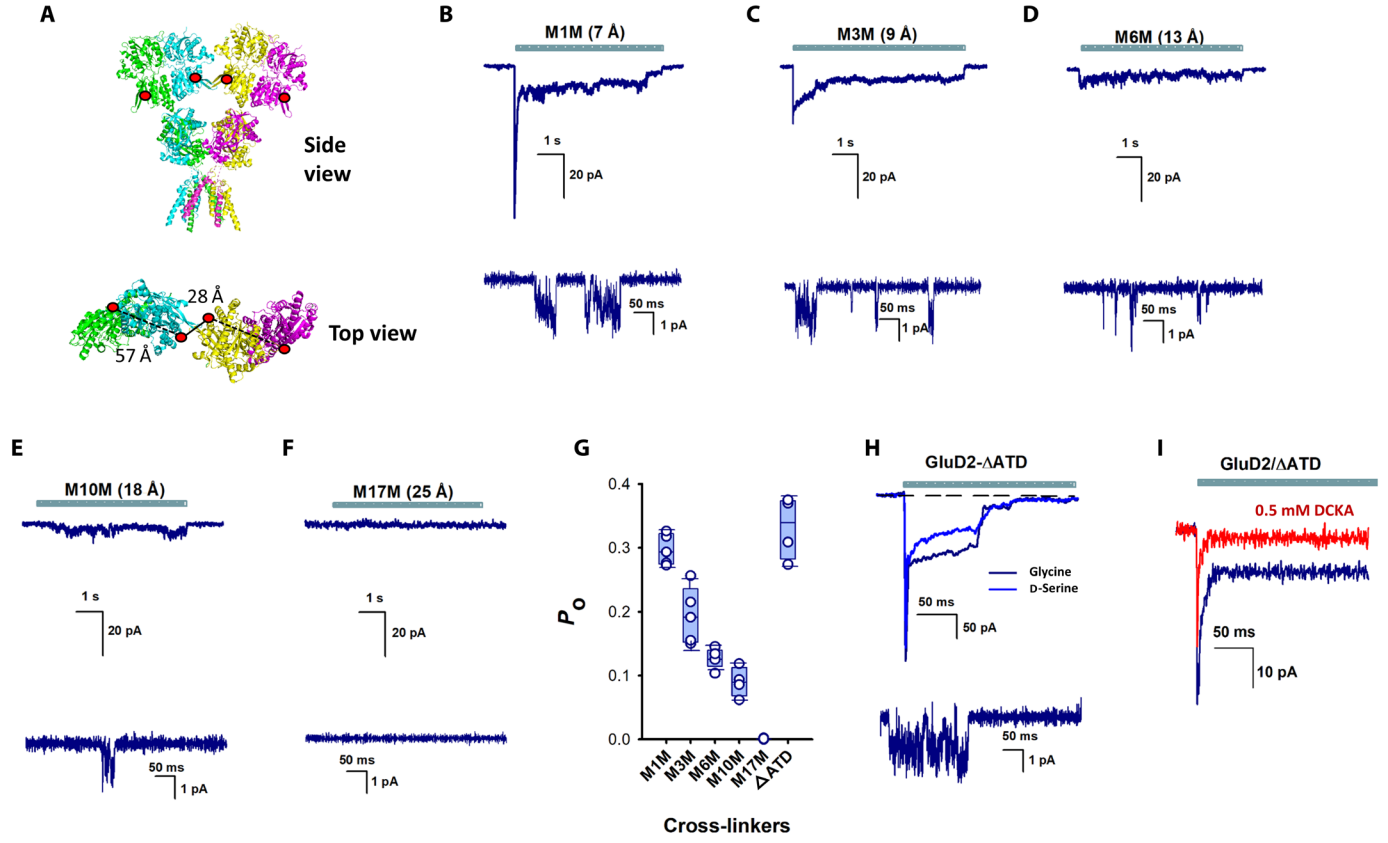

Fig. 5. N-terminal domain stabilization permits glycine activation of GluD2 receptors. (**A**) Structure of GluD2 (modeled on GluD1; PDB: 6KSS) showing the incorporation of a cysteine residue at position 276. Side view (top) and close-up top-down view of 207 N-terminal domain residues and distance between dimers (bottom). Representative whole-cell (top) and single-channel (bottom) currents evoked by glycine application in the presence of (**B**) 1,1-methanediyl bis-MTS (M1M), (**C**) 1,3-propanediyl bis-MTS (M3M), (**D**) 1,6-hexanediyl bis-MTS (M6M), (**E**) 1,10-decadiyl bis-MTS (M10M), and (**F**) 3,6,9,12,15-pentaoxaheptadecane-1,17-diyl bis-MTS (M17M). (**G**) Bar graphs showing probability of opening from at least three patches for the different cross-linkers and GluD2-ΔATD. (**H**) Representative glycine- and D-serine–evoked currents in GluD2 receptors lacking N-terminal domains. (**I**) Representative currents showing the inhibition of 10 mM glycine-mediated currents by 500 μM DCKA. ATD, amino terminal domain.

shown that, when the agonist-binding domain of GluD2 receptors was swapped with AMPA and kainate receptors, the receptor could be gated with glutamate (*41*). While these studies show the potential of the delta receptors to mediate ionotropic activity, the agonist-mediated currents have not been observed in these receptors.

The studies with the chimeric protein point to the extracellular domain of delta receptors as being responsible for the inability of these receptors to be agonist-gated ion channels (*41*). Structures of the GluD1 and GluD2 receptors also show that the largest difference between the delta receptors and the other subtypes of the ionotropic glutamate receptors is the large decoupling in the extracellular domains (*8*, *9*). This decoupling could be related to the nonswapped arrangement between the N-terminal domain and agonist-binding domain seen for the GluD1 and GluD2 receptors as opposed to domain swapping seen in the other subtypes of the mammalian ionotropic glutamate receptors. A similar nonswapped arrangement is seen in a plant ionotropic glutamate receptor (GLR3.4) that also exhibits extensive decoupling at the N-terminal domain (*42*). In the case of GLR3.4, binding of glutathione through *S*-glutathionylation of cysteine C205 was shown to cause a more closed clamshell, and this increased the currents mediated by the receptor due to agonist binding. In addition, GLR3.4 required the presence of auxiliary proteins CNIH1 and CN1H4 for activation with agonist. These studies with the GLR3.4 suggest that, when there is a nonswapped arrangement between the N-terminal domain and agonist-binding domain and large decoupling between subunits at the N-terminal domain, additional proteins and ligands are needed for the agonist to be able to mediate channel activation. These observations with GLR3.4 further support our study with GluD2 that show that the lack of agonist-mediated currents in the isolated receptors could be due to this decoupling observed in the extracellular domains of the isolated receptor. The need for conformational constraint in the extracellular domain for activation was also demonstrated by the cysteine cross-linking experiments with the GluD2 A654T Lurcher mutant (*13*). In this study, a cross-link was introduced at the agonist-binding domain dimer interface between sites P528 and L789 through introduction of cysteines, and the inherent C756-C811 disulfide bond was reduced by introducing the C811S mutation in the GluD2 A654T background. This mutant cross-linked protein showed activation by D-serine. The switch from inhibition by D-serine in the GluD2 A654T mutant receptor to activation in the cross-linked protein is similar to the results that we see in Fig. 2C, where glycine induces currents in GluD2 A654T mutant receptor in the presence of Clbn1 and NRX1 under cell-to-cell contact conditions. The prior cross-linking

studies further confirm our current investigations that indicate that restraining the dynamics in extracellular domain allows for channel activation.

In our study here, we show that GluD2 receptors show glycine- and D-serine–gated currents when studied in the context of cell-to-cell contact with Cbln1 and NRX1. On the basis of these electrophysiological measurements, fluorescence lifetimes that show tighter packing at the N-terminal domain in the presence of Cbln1 and NRX1, and chemical cross-linking experiments that show GluD2 receptor activity when the N-terminal domain is cross-linked, we propose that Cbln1 and NRX1 act as biological cross-linkers in GluD2. This tightly coupled receptor allows for the agonist-induced conformational changes in the ligand-binding domains to propagate to the transmembrane domains to activate (open) the ion channel (Fig. 6). These studies provide the first direct evidence that GluD2 delta receptors can form glycine- and D-serine–gated channels and function as ionotropic excitatory neurotransmitter receptors in situ, thus opening the field for further investigations.

MATERIALS AND METHODS

Cell culture, mutagenesis, and transfection

HEK-293T cells were maintained in Dulbecco's modified Eagle's medium (GenDEPOT), supplemented with 10% fetal bovine serum (GenDEPOT) and penicillin/streptomycin (Invitrogen/Life Technologies). The DNAs for GluD2, NRX1 [NRX1 AS4(+)], Cbln1, and Cbln4 were provided by M. Mishina, University of Tokyo, Tokyo. Mutations for GluD2 A654T (Lurcher mutant), GluD2-R275A/R276C mutant, and GluD2-ΔATD (Δ amino terminal domain) were introduced using standard polymerase chain reaction site-directed mutagenesis and confirmed by sequencing (Genewiz Inc.). Mutation for GluD2-SNAP was created by introducing SNAP tag (Addgene) after G301 of GluD2 using Gibson Assembly (New England Biolabs Inc.) and confirmed by sequencing (Genewiz Inc.). Transfections were performed using Lipofectamine 2000 (Invitrogen) with one of the homomeric GluD2 receptor subunits, A654T (Lurcher mutant), GluD2-R275A/R276C mutant, and GluD2-ΔATD along with green fluorescent protein (GFP), at a 1:0.2 ratio per 35-mm dish. To have a cluster transfection, we used HEK-293T cells at 80% confluency; in this condition, we mix GluD2, Nrx1, and Cbln1 or GluD2 A654T, Nrx1, and Cbln1 along with GFP at a 1:1:1:0.2 ratio.

Construct numbering is based on amino acid sequence ID: AAA17829.1 and includes the signal peptide. For mutations used in this study, cysteine for cross-linking was introduced at 276, R to C mutation was in the sequence VDVQELVRR, and SNAP tag was introduced between 301 and 302, corresponding to G and N in this sequence SQRCFRGN.

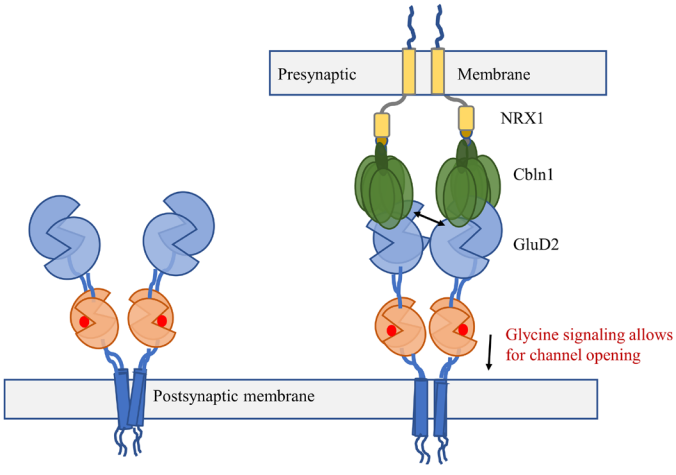

Fig. 6. Proposed mechanism of GluD2 activation. In the synapse when GluD2 is complexed with Cbln1 and NRX1, they act as biological cross-linkers to permit agonist-induced delta channel activation.

Whole-cell recordings

Patch-clamp experiments were performed in standard whole-cell configurations using an Axopatch 200B amplifier (Axon Instruments). Patch pipettes had a resistance of 3 to 5 megohms when filled with an internal solution consisting of 135 mM CsF, 33 mM CsCl, 2 mM $MgCl_2$, 1 mM $CaCl_2$, 11 mM EGTA, and 10 mM Hepes, adjusted to pH 7.4. The extracellular solution consisted of 150 mM NaCl, 1 mM $CaCl_2$, and 10 mM Hepes, adjusted to pH 7.4. External solutions were locally applied to lifted cells using a SF-77B perfusion fast-step (Warner Instruments). Currents were sampled at 50 or 10 kHz and filtered at 5 or 2 kHz with a 16-bit analog/digital converter (Axon Digidata 1550A, Axons Instruments) using pCLAMP 10 software (Molecular Devices). Whole-cell patch-clamp recordings were performed 24 to 48 hours after transfection, with a holding potential of −60 mV. For investigating the cells in clusters, the cells were grown to high confluency. For the electrophysiology recordings, cells that were surrounded by other cells through cell-to-cell contact were patched on the dish (fig. S2). Solution was perfused on to the cell, and cell-to-cell contact was maintained throughout the recording. For experiments without cell-to-cell contact, individual cells were lifted from the dish and moved closer to the perfusion tube (fig. S2).

Cross-linkers experiments

MTS compounds M1M, 1,3-propanediyl bis-MTS (M3M), 1,6-hexanediyl bis-MTS (M6M), and 1,10-decadiyl bis-MTS (M10M) were obtained from Toronto Research Chemicals, and 3,6,9,12,15-pentaoxaheptadecane-1,17-diyl bis-MTS (M17M) was obtained from Interchim. MTS compounds were obtained as powder and were dissolved in dimethyl sulfoxide, aliquoted, and kept on ice on the day of the experiment. HEK-293T cells expressing GluD2-R275A/R276C were incubated for 5 min, at low temperature, with 10 μM MTS compounds. After this exposure, the current in the cell was tested in the presence of 10 mM glycine. The cross-linker distances shown are distances between sulfur groups.

Single-channel recording

HEK-293T cells were plated in poly-D-lysine–coated 35-mm dishes and transfected 24 hours later, with GluD2-R275A/R276C mutant or GluD2-ΔATD constructs along with GFP at a 1:0.5 ratio. GluD2-R275A/R276C mutant construct was exposed to MTS compounds. Protocol used for the single-channel recordings have been described in (*43*); we performed the recordings in the outside out patch-clamp configuration, 24 hours after transfection. Patch pipettes had a resistance of 8 to 15 megohms when filled with an internal solution. Buffers and solution concentrations were similar to that used for whole-cell recordings. Data were acquired at 50 kHz and low pass filtered at 10 kHz (Axon Axopatch 200B and Digidata 1550A, Molecular Devices). The holding potential was −100 mV. Data were further filtered at 1 Hz.

Primary cerebellar and cortical neuron cultures

We use a similar protocol as previously described in (*43*). Animal procedures were approved by the University of Texas Health Science Center at Houston Animal Welfare Committee and were carried out in accordance with National Institutes of Health standards. The cortices of E-18 prenatal (Sprague-Dawley rats) embryos were dissected and dissociated by triturating as we previously described (*43*). We thank J. Aronowski for providing us with this. The dissociated cells were plated on poly-D-lysine– and laminin (Sigma-Aldrich)–coated glass coverslips, in Neurobasal medium with B27 at high density, and incubated in 5% CO_2 at 37°C. Half of the culture medium was changed every 2 days. After a total of 20 to 30 days in culture, the neuronal cells formed extensive axonal and dendritic networks (connections) and were ready for the electrophysiological experiments. To test physical synaptic connections in the cerebellar neurons, we recorded spontaneous EPSCs (sEPSCs) and spontaneous action potentials (fig. S7). Measurements of sEPSCs recordings were performed using the protocol described in (*43*); we used whole-cell voltage-clamp recordings in high cell density neurons culture at room temperature with a holding potential of −80 mV in the presence of tetrodotoxin (TTX), bicuculline, and Mg^{2+}. Also, the cerebellar neurons spontaneously fired action potentials when were studied in current clamp with physiological solutions. Spontaneous EPSCs and spontaneous action potentials were recorded at room temperature using an Axopatch 200B amplifier (Molecular Devices), acquired at 50 kHz using pCLAMP10 software (Molecular Devices), and filtered online at 5 kHz. The buffers used for the studies are similar to that used by Carrillo *et al.* (*43*), and internal solution consisted of the following: 120 mM Cs-gluconate, 20 mM Hepes, 4 mM $MgCl_2$, 10 mM EGTA, 0.4 mM guanosine 5′-triphosphate (GTP)–Na, 4 mM adenosine 5′-triphosphate (ATP)–Mg, and 5 mM phosphocreatine (pH 7.3). The external solution was consisted of the following: 150 mM NaCl, 4 mM KCl, 2 mM $CaCl_2$, 2 mM $MgCl_2$, 10 mM Hepes, 50 mM D,L-2-amino-5-phosphonovaleric acid, 10 μM bicuculline, and 1 mM TTX (pH 7.4). For the spontaneous action potentials, the internal solution was consisted of the following: 120 mM KCl, 20 mM Hepes, 4 mM $MgCl_2$, 10 mM EGTA, 0.4 mM GTP-Na, 4 mM ATP-Mg, and 5 mM phosphocreatine (pH 7.3). The external solution was consisted of the following: 150 mM NaCl, 4 mM KCl, 2 mM $CaCl_2$, 2 mM $MgCl_2$, and 10 mM Hepes.

For experiments with connections, we recorded by patching the neurons on the dish without disrupting the networks. For experiments without contacts, individual neurons from 2 to 3 days of culture were lifted from the dish and moved closer to the perfusion tube (fig. S2).

The neuron recordings were performed in whole-cell patch clamp configuration at room temperature, with a holding potential of −80 mV. Patch pipettes had a resistance of 8 to 15 megohms when filled with an internal solution consisting of 120 mM Cs-gluconate, 20 mM Hepes, 4 mM $MgCl_2$, 10 mM EGTA, 0.4 mM GTP-Na, 4 mM ATP-Mg, and 5 mM phosphocreatine, adjusted to pH 7.3. The extracellular solution consisted of 150 mM NaCl, 4 mM KCl, 2 mM $CaCl_2$, 2 mM $MgCl_2$, and 10 mM Hepes, adjusted to pH 7.4. To isolate GluD2 currents, 1 μM tetrodotoxin, 10 μM bicuculline, 10 μM NBQX, 1 μM strychnine, and 100 μM DL-AP5 were added to the extracellular solution.

Fluorescence lifetime imaging

HEK-293T cells were plated in poly-D-lysine–coated glass coverslips and transfected 24 hours later with GluD2-SNAP or GluD2-SNAP, Nrx1, and Cbln1 constructs. To measure FLIM, GluD2-SNAP was labeled with photostable fluorescent substrates SNAP-Surface 649 and SNAP-Surface Alexa Fluor 546 (New England Biolabs). The experiments were performed after 48 hours of transfection. The cells were washed three times with extracellular buffer solution (145 mM NaCl, 1 mM CaCl2, 3 mM KCl, 10 mM Hepes, and 10 mM glucose), incubated with 2.5 μM fluorescent substrates, and placed back in the incubator for a 2-hour period. After incubation, the cells were washed three times with extracellular buffer solution, and imaging experiments were performed.

For FLIM imaging, a MicroTime 200 confocal fluorescence microscope (PicoQuant, Berlin, Germany) was used, consisting of an inverted microscope (IX73, Olympus) equipped with an Olympus PlanApo 100×/numerical aperture 1.4 oil immersion objective. Fluorescence recordings were performed in the time-correlated single-photon counting mode using single-photon sensitive detectors (PicoQuant, Berlin, Germany). A 530-nm pulsed laser diode was used for excitation, band pass filter of 582/64 nm was used to measure donor emission, and band pass filter of 690/70 nm was used to measure acceptor emission. Data acquisition and analysis were performed by the SymPhoTime 64 software version 2.4 (PicoQuant, Berlin, Germany). The photons from the plasma membranes of the cells were selected to obtain the fluorescence intensity decay. The fluorescence intensity decays were analyzed using SigmaPlot. Data from 3 days were used to obtain mean and SE values for the lifetimes.

Data analysis

Following the procedure previously described in (*43*), we performed data analysis with Clampfit 10 (Axon Instruments) and SymPhoTime 64. At least three recordings were obtained for each condition studied from at least three different days. Concentration-response curves showing steady-state stimulation as a function of agonist concentrations were fit to the Hill equation

$$I = (I_{\min} + (I_{\max} - I_{\min}))/((1 + 10\text{^}n(\log EC50 - C))$$

where I is steady state current, $I_{\min}$ is the lowest value for steady state stimulation, $I_{\max}$ is the maximum value for steady state stimulation, EC_{50} is concentration of agonist at half-maximal stimulation, and C is the concentration of agonist.

All electrophysiological and imaging data were statistically analyzed with the Student's paired t test, with significance taken as $P < 0.05$. These tests were performed using GraphPad Prism software (GraphPad Software).

SUPPLEMENTARY MATERIALS

Supplementary material for this article is available at https://science.org/doi/10.1126/sciadv.abk2200

View/request a protocol for this paper from *Bio-protocol*.

REFERENCES AND NOTES

1. S. F. Traynelis, L. P. Wollmuth, C. J. McBain, F. S. Menniti, K. M. Vance, K. K. Ogden, K. B. Hansen, H. Yuan, S. J. Myers, R. Dingledine, Glutamate receptor ion channels: Structure, regulation, and function. *Pharmacol. Rev.* **62**, 405–496 (2010).
2. G. J. Iacobucci, G. K. Popescu, NMDA receptors: Linking physiological output to biophysical operation. *Nat. Rev. Neurosci.* **18**, 236–249 (2017).
3. S. M. Schmid, M. Hollmann, To gate or not to gate: Are the delta subunits in the glutamate receptor family functional ion channels? *Mol. Neurobiol.* **37**, 126–141 (2008).
4. J. Elegheert, W. Kakegawa, J. E. Clay, N. F. Shanks, E. Behiels, K. Matsuda, K. Kohda, E. Miura, M. Rossmann, N. Mitakidis, J. Motohashi, V. T. Chang, C. Siebold, I. H. Greger,

T. Nakagawa, M. Yuzaki, A. R. Aricescu, Structural basis for integration of GluD receptors within synaptic organizer complexes. *Science* **353**, 295–299 (2016).
5. S. Cheng, A. B. Seven, J. Wang, G. Skiniotis, E. Özkan, Conformational plasticity in the transsynaptic neurexin-cerebellin-glutamate receptor adhesion complex. *Structure* **24**, 2163–2173 (2016).
6. K. Matsuda, E. Miura, T. Miyazaki, W. Kakegawa, K. Emi, S. Narumi, Y. Fukazawa, A. Ito-Ishida, T. Kondo, R. Shigemoto, M. Watanabe, M. Yuzaki, Cbln1 is a ligand for an orphan glutamate receptor δ2, a bidirectional synapse organizer. *Science* **328**, 363–368 (2010).
7. K. Suzuki, J. Elegheert, I. Song, H. Sasakura, O. Senkov, K. Matsuda, W. Kakegawa, A. J. Clayton, V. T. Chang, M. Ferrer-Ferrer, E. Miura, R. Kaushik, M. Ikeno, Y. Morioka, Y. Takeuchi, T. Shimada, S. Otsuka, S. Stoyanov, M. Watanabe, K. Takeuchi, A. Dityatev, A. R. Aricescu, M. Yuzaki, A synthetic synaptic organizer protein restores glutamatergic neuronal circuits. *Science* **369**, eabb4853 (2020).
8. A. P. Burada, R. Vinnakota, J. Kumar, The architecture of GluD2 ionotropic delta glutamate receptor elucidated by cryo-EM. *J. Struct. Biol.* **211**, 107546 (2020).
9. A. P. Burada, R. Vinnakota, J. Kumar, Cryo-EM structures of the ionotropic glutamate receptor GluD1 reveal a non-swapped architecture. *Nat. Struct. Mol. Biol.* **27**, 84–91 (2020).
10. A. C. Chin, R. A. Yovanno, T. J. Wied, A. Gershman, A. Y. Lau, D-serine potently drives ligand-binding domain closure in the ionotropic glutamate receptor GluD2. *Structure* **28**, 1168–1178.e2 (2020).
11. A. S. Kristensen, K. B. Hansen, P. Naur, L. Olsen, N. L. Kurtkaya, S. M. Dravid, T. Kvist, F. Yi, J. Pøhlsgaard, R. P. Clausen, M. Gajhede, J. S. Kastrup, S. F. Traynelis, Pharmacology and structural analysis of ligand binding to the orthosteric site of glutamate-like GluD2 receptors. *Mol. Pharmacol.* **89**, 253–262 (2016).
12. P. Naur, K. B. Hansen, A. S. Kristensen, S. M. Dravid, D. S. Pickering, L. Olsen, B. Vestergaard, J. Egebjerg, M. Gajhede, S. F. Traynelis, J. S. Kastrup, Ionotropic glutamate-like receptor delta2 binds D-serine and glycine. *Proc. Natl. Acad. Sci. U.S.A.* **104**, 14116–14121 (2007).
13. K. B. Hansen, P. Naur, N. L. Kurtkaya, A. S. Kristensen, M. Gajhede, J. S. Kastrup, S. F. Traynelis, Modulation of the dimer interface at ionotropic glutamate-like receptor delta2 by D-serine and extracellular calcium. *J. Neurosci.* **29**, 907–917 (2009).
14. J. Zuo, P. L. de Jager, K. A. Takahashi, W. Jiang, D. J. Linden, N. Heintz, Neurodegeneration in Lurcher mice caused by mutation in delta2 glutamate receptor gene. *Nature* **388**, 769–773 (1997).
15. L. P. Wollmuth, T. Kuner, C. Jatzke, P. H. Seeburg, N. Heintz, J. Zuo, The Lurcher mutation identifies delta 2 as an AMPA/kainate receptor-like channel that is potentiated by Ca(2+). *J. Neurosci.* **20**, 5973–5980 (2000).
16. V. Ady, J. Perroy, L. Tricoire, C. Piochon, S. Dadak, X. Chen, I. Dusart, L. Fagni, B. Lambolez, C. Levenes, Type 1 metabotropic glutamate receptors (mGlu1) trigger the gating of GluD2 delta glutamate receptors. *EMBO Rep.* **15**, 103–109 (2014).
17. D. Lemoine, S. Mondoloni, J. Tange, B. Lambolez, P. Faure, A. Taly, L. Tricoire, A. Mourot, Probing the ionotropic activity of glutamate GluD2 receptor in HEK cells with genetically-engineered photopharmacology. *eLife* **9**, e59026 (2020).
18. J. Baranovic, A. J. Plested, Auxiliary subunits keep AMPA receptors compact during activation and desensitization. *eLife* **7**, e40548 (2018).
19. L. G. Zachariassen, L. Katchan, A. G. Jensen, D. S. Pickering, A. J. R. Plested, A. S. Kristensen, Structural rearrangement of the intracellular domains during AMPA receptor activation. *Proc. Natl. Acad. Sci. U.S.A.* **113**, E3950–E3959 (2016).
20. J. Gonzalez, M. Du, K. Parameshwaran, V. Suppiramaniam, V. Jayaraman, Role of dimer interface in activation and desensitization in AMPA receptors. *Proc. Natl. Acad. Sci. U.S.A.* **107**, 9891–9896 (2010).
21. E. Carrillo, S. A. Shaikh, V. Berka, R. J. Durham, D. B. Litwin, G. Lee, D. M. MacLean, L. M. Nowak, V. Jayaraman, Mechanism of modulation of AMPA receptors by TARP-γ8. *J. Gen. Physiol.* **152**, e201912451 (2020).
22. S. A. Shaikh, D. M. Dolino, G. Lee, S. Chatterjee, D. M. MacLean, C. Flatebo, C. F. Landes, V. Jayaraman, Stargazin modulation of AMPA receptors. *Cell Rep.* **17**, 328–335 (2016).
23. L. Mony, S. Zhu, S. Carvalho, P. Paoletti, Molecular basis of positive allosteric modulation of GluN2B NMDA receptors by polyamines. *EMBO J.* **30**, 3134–3146 (2011).
24. R. E. Sirrieh, D. M. MacLean, V. Jayaraman, Subtype-dependent N-methyl-D-aspartate receptor amino-terminal domain conformations and modulation by spermine. *J. Biol. Chem.* **290**, 12812–12820 (2015).
25. M. B. Warf, M. Nakamori, C. M. Matthys, C. A. Thornton, J. A. Berglund, Pentamidine reverses the splicing defects associated with myotonic dystrophy. *Proc. Natl. Acad. Sci. U.S.A.* **106**, 18551–18556 (2009).
26. G. Benaim, C. Lopez-Estraño, R. Docampo, S. N. Moreno, A calmodulin-stimulated Ca^{2+} pump in plasma-membrane vesicles from Trypanosoma brucei; selective inhibition by pentamidine. *Biochem. J.* **296**(Pt. 3), 759–763 (1993).
27. S. Sarkar, M. D. Berry, Involvement of organic cation transporter 2 and a Na(+)-dependent active transporter in p-tyramine transport across Caco-2 intestinal cells. *Life Sci.* **253**, 117696 (2020).
28. Y. Kitamura, T. Arima, R. Imaizumi, T. Sato, Y. Nomura, Inhibition of constitutive nitric oxide synthase in the brain by pentamidine, a calmodulin antagonist. *Eur. J. Pharmacol.* **289**, 299–304 (1995).
29. F. Taverna, Z. G. Xiong, L. Brandes, J. C. Roder, M. W. Salter, J. F. MacDonald, The Lurcher mutation of an α-amino-3-hydroxy-5-methyl- 4-isoxazolepropionic acid receptor subunit enhances potency of glutamate and converts an antagonist to an agonist. *J. Biol. Chem.* **275**, 8475–8479 (2000).
30. C. Nakamoto, K. Konno, T. Miyazaki, E. Nakatsukasa, R. Natsume, M. Abe, M. Kawamura, Y. Fukazawa, R. Shigemoto, M. Yamasaki, K. Sakimura, M. Watanabe, Expression mapping, quantification, and complex formation of GluD1 and GluD2 glutamate receptors in adult mouse brain. *J. Comp. Neurol.* **528**, 1003–1027 (2020).
31. K. Araki, H. Meguro, E. Kushiya, C. Takayama, Y. Inoue, M. Mishina, Selective expression of the glutamate receptor channel delta 2 subunit in cerebellar Purkinje cells. *Biochem. Biophys. Res. Commun.* **197**, 1267–1276 (1993).
32. M. Yuzaki, Cerebellar LTD vs. motor learning-lessons learned from studying GluD2. *Neural Netw.* **47**, 36–41 (2013).
33. G. E. Utine, G. Haliloğlu, B. Salancı, A. Çetinkaya, P. Ö. Kiper, Y. Alanay, D. Aktaş, K. Boduroğlu, M. Alikaşifoğlu, A homozygous deletion in GRID2 causes a human phenotype with cerebellar ataxia and atrophy. *J. Child Neurol.* **28**, 926–932 (2013).
34. L. B. Hills, A. Masri, K. Konno, W. Kakegawa, A. T. N. Lam, E. Lim-Melia, N. Chandy, R. S. Hill, J. N. Partlow, M. al-Saffar, R. Nasir, J. M. Stoler, A. J. Barkovich, M. Watanabe, M. Yuzaki, G. H. Mochida, Deletions in GRID2 lead to a recessive syndrome of cerebellar ataxia and tonic upgaze in humans. *Neurology* **81**, 1378–1386 (2013).
35. T. A. Greenwood, L. C. Lazzeroni, S. S. Murray, K. S. Cadenhead, M. E. Calkins, D. J. Dobie, M. F. Green, R. E. Gur, R. C. Gur, G. Hardiman, J. R. Kelsoe, S. Leonard, G. A. Light, K. H. Nuechterlein, A. Olincy, A. D. Radant, N. J. Schork, L. J. Seidman, L. J. Siever, J. M. Silverman, W. S. Stone, N. R. Swerdlow, D. W. Tsuang, M. T. Tsuang, B. I. Turetsky, R. Freedman, D. L. Braff, Analysis of 94 candidate genes and 12 endophenotypes for schizophrenia from the Consortium on the Genetics of Schizophrenia. *Am. J. Psychiatry* **168**, 930–946 (2011).
36. M. Orsetti, F. Di Brisco, P. L. Canonico, A. A. Genazzani, P. Ghi, Gene regulation in the frontal cortex of rats exposed to the chronic mild stress paradigm, an animal model of human depression. *Eur. J. Neurosci.* **27**, 2156–2164 (2008).
37. W. Kakegawa, T. Miyazaki, K. Emi, K. Matsuda, K. Kohda, J. Motohashi, M. Mishina, S. Kawahara, M. Watanabe, M. Yuzaki, Differential regulation of synaptic plasticity and cerebellar motor learning by the C-terminal PDZ-binding motif of GluRdelta2. *J. Neurosci.* **28**, 1460–1468 (2008).
38. W. Kakegawa, T. Miyazaki, K. Kohda, K. Matsuda, K. Emi, J. Motohashi, M. Watanabe, M. Yuzaki, The N-terminal domain of GluD2 (GluRdelta2) recruits presynaptic terminals and regulates synaptogenesis in the cerebellum in vivo. *J. Neurosci.* **29**, 5738–5748 (2009).
39. W. Kakegawa, Y. Miyoshi, K. Hamase, S. Matsuda, K. Matsuda, K. Kohda, K. Emi, J. Motohashi, R. Konno, K. Zaitsu, M. Yuzaki, D-serine regulates cerebellar LTD and motor coordination through the δ2 glutamate receptor. *Nat. Neurosci.* **14**, 603–611 (2011).
40. S. C. Gantz, K. Moussawi, H. S. Hake, Delta glutamate receptor conductance drives excitation of mouse dorsal raphe neurons. *eLife* **9**, e56054 (2020).
41. S. M. Schmid, S. Kott, C. Sager, T. Huelsken, M. Hollmann, The glutamate receptor subunit delta2 is capable of gating its intrinsic ion channel as revealed by ligand binding domain transplantation. *Proc. Natl. Acad. Sci. U.S.A.* **106**, 10320–10325 (2009).
42. M. N. Green, S. P. Gangwar, E. Michard, A. A. Simon, M. T. Portes, J. Barbosa-Caro, M. M. Wudick, M. A. Lizzio, O. Klykov, M. V. Yelshankaya, J. A. Feijó, A. I. Sobolevsky, Structure of the *Arabidopsis thaliana* glutamate receptor-like channel GLR3.4. *Mol. Cell* **81**, 3216–3226.e8 (2021).
43. E. Carrillo, N. K. Bhatia, A. M. Akimzhanov, V. Jayaraman, Activity dependent inhibition of AMPA receptors by Zn^{2+}. *J. Neurosci.* **40**, 8629–8636 (2020).

Acknowledgments: We thank N. K. Bhatia for help with cloning, R. Durham for help with editing, and P. C. Flores for the illustration in Fig. 2A. **Funding:** This work was supported by the National Institutes of Health grant R35 GM122528 to V.J., American Heart Association Fellowship 18POST34030189 to E.C., and Training Interdisciplinary Pharmacology Scientists (TIPS) Program Grant fellowship T32 GM120011 to C.U.G. **Author contributions:** Conceptualization: V.J. and E.C. Methodology: E.C., C.U.G., V.B., and V.J. Molecular cloning: C.U.G. Data acquisition: E.C. and V.B. Data analysis: E.C., V.B., and V.J. Supervision: V.J. Writing (original draft): E.C. Writing (review and editing): E.C. and V.J. **Competing interests:** The authors declare that they have no competing interests. **Data and materials availability:** All data needed to evaluate the conclusions in the paper are present in the paper and/or the Supplementary Materials.

Submitted 29 June 2021
Accepted 3 November 2021
Published 22 December 2021
10.1126/sciadv.abk2200